Sensors and Actuators A 280 (2018) 303–308

Contents lists available at ScienceDirect

Sensors and Actuators A: Physical

journal homepage: www.elsevier.com/locate/sna

An air-spaced terahertz metamaterial perfect absorber

Guangwu Duan [a], Jacob Schalch [b], Xiaoguang Zhao [a], Jingdi Zhang [b], Richard D. Averitt [b,*], Xin Zhang [a,*]

[a] Department of Mechanical Engineering, Boston University, Boston, MA 02215, USA
[b] Department of Physics, University of California, San Diego, La Jolla, CA 92093, USA

ARTICLE INFO

Article history:
Received 30 September 2017
Received in revised form 18 May 2018
Accepted 26 July 2018
Available online 29 July 2018

Keywords:
Air-spacer
Metamaterials
Metamaterial perfect absorber
Terahertz
High quality factor
High sensitivity

ABSTRACT

Metamaterial absorbers are typically comprised of a layer of split-ring resonators and a ground plane with a dielectric spacer layer that provides structural support and in which absorbed energy is deposited. We address the question "What happens to the absorption if the spacer layer is removed?" through the design, fabrication, and characterization of a terahertz metamaterial absorber with air as the spacer layer. Reflection based terahertz time-domain spectroscopy was employed to measure the absorption and interference theory was used to interpret the results. The surface current in the gold ground plane and split-ring resonator layer is solely responsible for the absorption in the form of joule heating. In comparison to dielectric spacer layer absorbers, the quality factor is increased by a factor of ~3. The electric field is highly concentrated in the volume between split-ring resonator layer and the ground plane offering the potential for novel sensing application if materials can be incorporated into this region (e.g. with microfluidics). In the spirit of this possibility, simulations of the absorption have been performed. The variation of the real part of the permittivity of the spacer material results in an absorption peak frequency shift, while a change in the imaginary part affects the quality factor and amplitude. Ultimately, the high quality factor and the absence of the spacer material provide the air-spacer metamaterial absorber with unique advantages for sensing applications.

1. Introduction

Metamaterials are engineered subwavelength structures exhibiting extraordinary electromagnetic properties when resonantly excited by electromagnetic fields [1–3]. Metamaterial perfect absorbers were originally reported as two metamaterial layers patterned with split-ring resonators (SRRs) and cut-wires separated by an intervening dielectric spacer [4,5]. Subsequently, a pure ground plane was employed to replace one of the metamaterial layers [6]. With judicious design and fabrication, it is possible to realize near-unity absorption at a well-defined frequency. Similar configuration was also developed in microwave range known as circuit-analog absorber. The concept is, however, rarely extended to other frequencies, and the thickness is usually around a quarter of the wavelength [7,8]. For the metamaterial perfect absorbers, a widely accepted explanation for near-unity absorption is effective medium theory [5] where the effective permittivity and permeability are separately tuned to match the free space impedance thereby minimizing the reflected light (the transmission is zero because of the ground plane, meaning the absorption is ~1). Another well-established approach is transmission line theory [9,10], which considers the metamaterial absorber as a one-port shorted transmission line from which it is possible to retrieve the equivalent impedance. Recently, it has been found that if the coupling between the metamaterials and the ground plane is negligible (reasonable for typical spacer layer thicknesses), the total reflection can be modeled as the superposition of the multiple reflections caused by the two metallic layers using interference theory [11].

Metamaterial absorbers can potentially be employed in imaging, sensing and detection applications, amongst others [12,13]. The spacer material is an essential component of a metamaterial absorber and its precise design (in terms of thickness and dielectric function) is critical towards realizing a variety of applications. For example, the spacer can be partially etched and replaced with liquid crystals to realize an electrically tunable metamaterial absorber [14]. Alternatively, by utilizing VO_2 as the spacer material, the absorption resonance can be switched on and off [15] with tem-

* Corresponding author.
E-mail addresses: raveritt@ucsd.edu (R.D. Averitt), xinz@bu.edu (X. Zhang).

https://doi.org/10.1016/j.sna.2018.07.052
0924-4247/

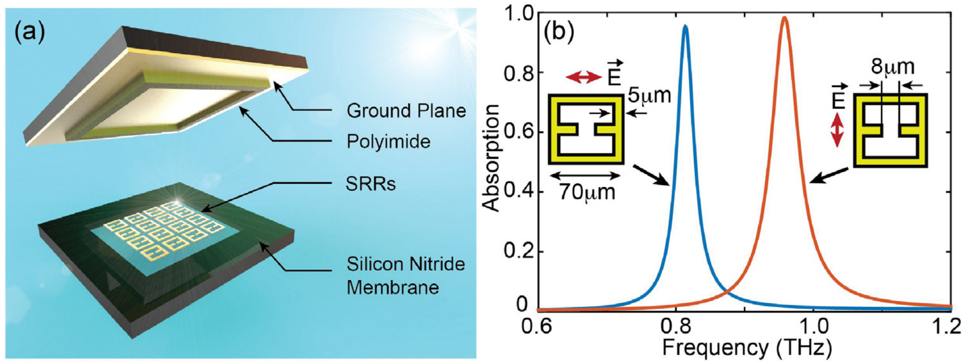

Fig. 1. (a) Schematic drawing of the assembling of the air-spacer absorber. (b) Simulated absorption spectra with incident THz pulse polarized as the insets. The side length of the SRRs is 70 μm, the line width is 5 μm, and the gap is 8 μm.

perature switching of the insulator-to-metal transition. Moreover, by integrating semiconductor material within the spacer, nonlinear properties can be introduced [16]. Importantly, the quality factor of metamaterial absorbers is typically higher than single layers of metamaterials [11], and is therefore more suitable for sensing applications. However, the physical presence of the dielectric spacer material precludes access to the volume between the metamaterial layer and the ground plane, where the electric field is highly concentrated. Additionally, dielectric loss of the spacer material can reduce the quality factor.

2. Design and fabrication

In this paper, we designed, fabricated, and characterized a metamaterial absorber with an air-spacer, demonstrating the near-unity absorption remains achievable with a measured quality factor of 19.8 which is larger than counterpart dielectric spacer absorbers by a factor of ∼3. Additionally, the absence of the spacer material yields the possibility to access the space between the SRR layer and the ground plane. The advantages introduced above provide the air-spacer metamaterial absorber with a unique opportunity to be configured for sensing applications or to realize a larger degree of tunability.

A schematic drawing of our metamaterial absorber design is shown in Fig. 1(a). An array of SRRs (150 nm thick) was patterned on a silicon nitride (0.4 μm thick) membrane and flip chip bonded to a ground plane with polyimide as the adhesion layer (thickness of 5 μm) at the perimeter of the array. The geometry of the SRRs is introduced in the caption of Fig. 1 and the periodicity of the array is 80 μm. The absorption spectrum was simulated using CST Microwave Studio 2016 with unit cell boundary condition. The permittivity of the silicon nitride membrane was set as $\varepsilon_{SiN} = 7.6 + i0.04$ [17]. Gold was set as lossy metal with a conductivity of 4.56×10^7 S/m, and the background was set as vacuum. The simulated absorption spectra are plotted in Fig. 1(b) with the incident terahertz (THz) pulse polarized parallel (blue) or perpendicular (red) to the gap exhibiting absorption peaks at 0.812 THz and 0.958 THz, respectively.

The fabrication of the structure layer began with a double-side silicon nitride coated silicon wafer. SRRs were patterned using a lift off process using photolithography and e-beam evaporation. Next, the backside silicon nitride membrane was patterned with open windows and etched by reactive ion etching as the mask for the following wet etching, in which KOH solution was applied to completely remove the silicon in the window areas, leaving only the top side silicon nitride membranes with patterned SRRs. A second wafer was coated with 150 nm thick gold as the ground plane, on which 10 μm thick polyimide (HD8820) was spin coated and photolithographed. Finally, the structure layer and the ground plane were flip chip bonded by applying high temperature (175 °C) and force (200 g). The thickness of the air-spacer was measured as 5 μm using a microscope with digital dial indicator. Fig. 2(a) and (b) show the image of a fabricated air-spacer absorber and the microscopy image of the unit cell array [18].

3. Characterization and analysis

3.1. Device characterization

The sample was characterized using THz time-domain spectroscopy at normal incidence in reflection. The time domain reflection signal was measured, Fourier transformed to the frequency domain, and normalized to the reference signal measured with a gold mirror. Due to the zero transmission through the metallic ground plane, the absorber spectrum can be expressed as $A = 1 - |r|^2$, where A is the amplitude of absorption and r is the field reflection coefficient. The experimental absorption spectra with incident THz pulse polarized parallel and perpendicular to the SRRs capacitive gaps are plotted in Fig. 3(a) and (b). The x–y plane is defined parallel to the metamaterial layer with x direction along the gap, y direction perpendicular to the gap, and z direction perpendicular to the metamaterial layer as shown by the inset in Fig. 3. Absorption peaks were observed at the frequency of 0.811 THz for parallel polarization and 0.954 THz for perpendicular polarization with amplitude of 88.4% and 99.8%, respectively. The experimental results (solid blue curves) show a high degree of agreement with the simulation results (dashed red curves). The slight mismatch is possibly caused by the deformation of the silicon nitride membrane, or misalignment of the gap to the polarization direction during the testing. The theoretical results based on interference theory are also depicted in Fig. 3 as the green curves, which will be discussed later.

3.2. Analysis based on interference theory

Interference theory was employed to analyze the absorption, which considers the total reflection as the superposition of the multiple reflections between the metamaterials and the ground plane. A model including only a single layer of SRRs on a silicon nitride membrane was simulated to retrieve the reflection and transmission coefficients (amplitude and phase). Using this information, the reflection spectrum was calculated using the following equation [11]:

$$r = r_{12} - \frac{t_{12}t_{21}}{r_{21} + e^{-i2\beta}} \tag{1}$$

where r is the total reflection coefficient, r_{12}, t_{12} and r_{21}, t_{21} are the reflection and transmission coefficients from the air to the silicon nitride membrane side or to the SRRs side, $\beta = n\,k\,d$ is the one-way

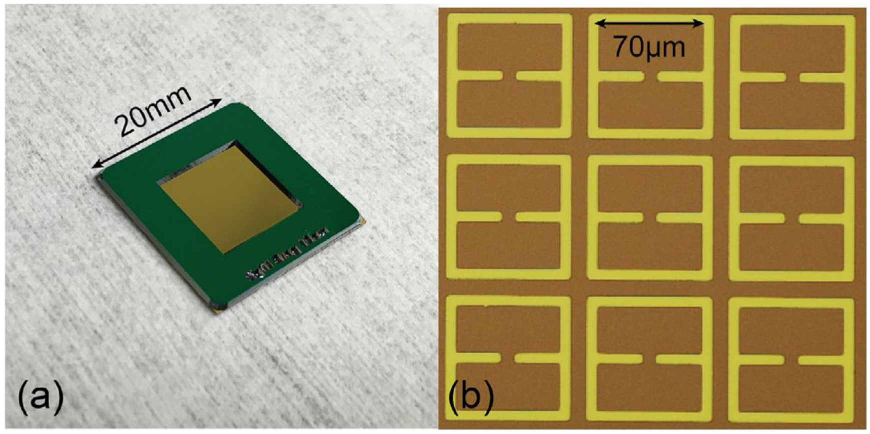

Fig. 2. (a) Image of a fabricated air-spacer metamaterial absorber with side length of 20 mm. (b) The microscopy image of the unit cell array.

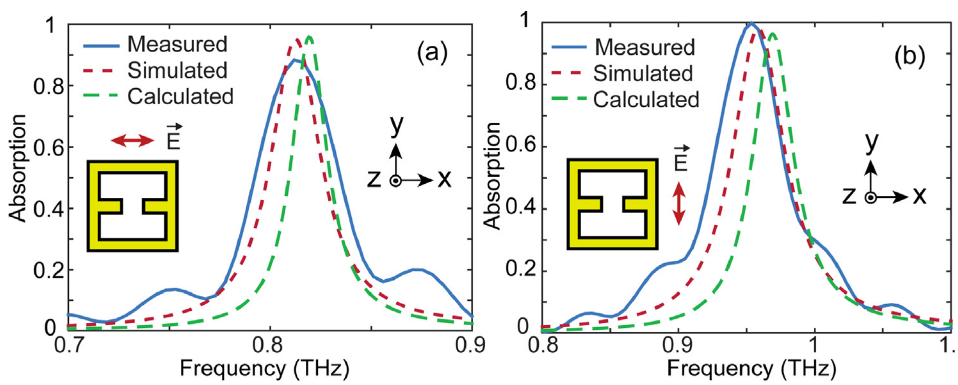

Fig. 3. Absorption spectra comparison amongst experimental, simulation, and theoretical results for incident THz pulse polarized (a) parallel and (b) perpendicular to the gap. The polarization of the incident pulse is indicated with red arrow in the inset. (For interpretation of the references to colour in this figure legend, the reader is referred to the web version of this article).

phase delay in the spacer, and *n*, *k*, *d* are the refractive index of the spacer material, the wave number in vacuum, and the thickness of the spacer, respectively. The theoretical results are plotted in Fig. 3 as the green dashed curve. Compared with the experimental results, a slight blue shift of the absorption peak frequencies is observed. The frequency mismatch between the experimental and theoretical results were 0.007 THz and 0.016 THz for LC and dipole absorption modes respectively, which were 0.9% and 1.7% offset of the absorption peak frequencies. The mismatch is caused by neglecting the coupling between the metamaterials and the ground plane in the parameter retrieval process, which contributed as an enhanced mutual capacitance. This neglect can result in an absorption peak frequency higher than the experiment results [19,20].

3.3. Analysis of the power dissipation

For traditional metamaterial absorbers with a dielectric material as the spacer layer, significant absorption occurs within the dielectric (depending of course on the magnitude of the imaginary part of the dielectric function) [21]. With an air-spacer metamaterial perfect absorber, the absorption must occur solely in the metal layers and thin silicon nitride supporting layer. To investigate this in detail, the power loss in each layer of the absorber was simulated using CST Microwave Studio 2016. At the absorption peak frequencies, the simulated power dissipation in silicon nitride, ground plane, and the SRRs are 5.3%, 18.6%, and 76.1% for LC absorption mode, and 6.0%, 17.9%, and 76.1% for dipole absorption mode. Thus, the surface current in the SRRs and the ground plane contribute most to the absorption in the form of joule heating. Based on the surface current depicted in Fig. 4, the power consumption primarily occurred at the sides labeled 1 and 2 parallel to the gap for the LC absorption mode, while for the dipole absorption mode the primary power consumption occurred at the sides labeled 3 and 4 perpendicular to the gap. More importantly, the reduction of the dielectric loss increases quality factor. For the measurement and simulation results, the quality factors are 19.8 and 28.2 for LC absorption mode, and 17.2 and 21.02 for dipole absorption mode, calculated by dividing the peak frequency by the full width at half maximum. The differences between the experimental and simulated quality factors may be due to the non-uniformity of the fabricated unit cells. The quality factor can be further increased by improving the fabrication techniques to achieve higher uniformity of the unit cells and the spacer thickness across the whole sample and by reducing ohmic loss in metallic structures. Nevertheless, comparing with reported metamaterial absorbers using polyimide spacers, the quality factor is increased in excess of threefold [16,22].

3.4. Analysis of magnetic and electric field distribution

To understand the character of the resonant absorption, simulations of the *z*-component of the magnetic field strength in the *x*–*y* plane at the middle of the spacer layer are depicted in Fig. 4(a) and (b) for the incident THz pulse polarized parallel and perpendicular

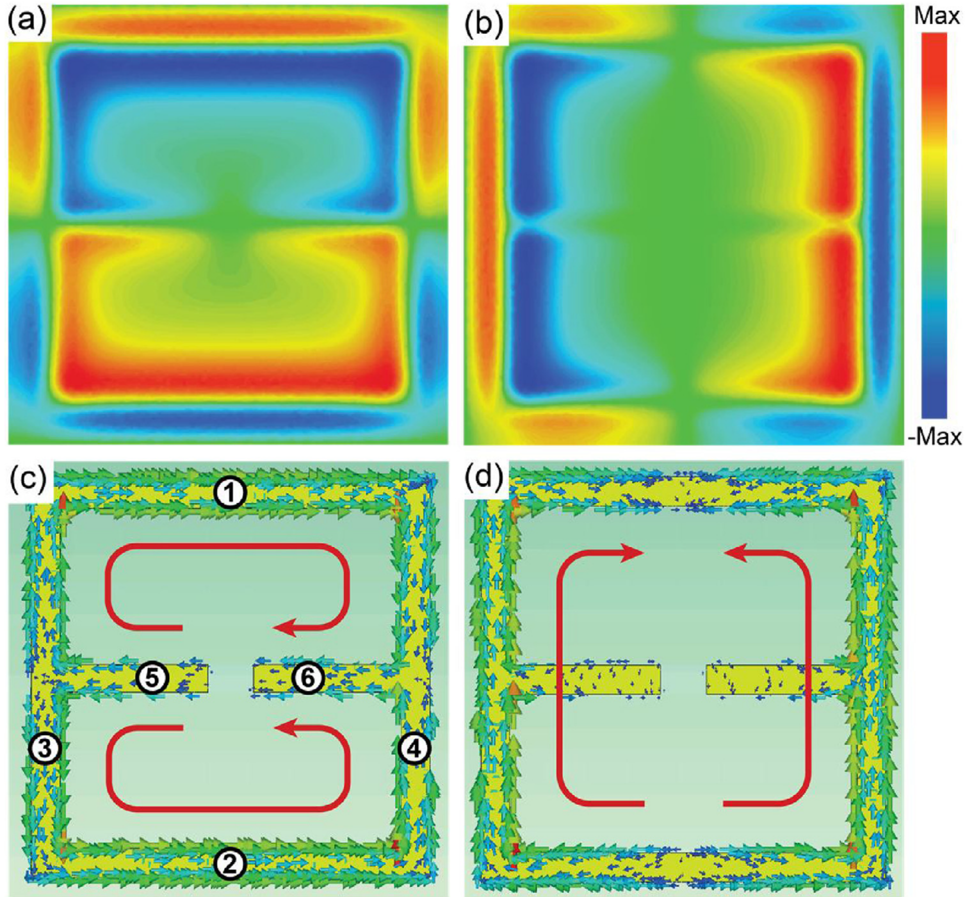

Fig. 4. The simulated magnetic field distribution along *z*-direction at the middle cross section of the spacer with incident wave polarized (a) parallel and (b) perpendicular to the gap, and the corresponding surface current in (c) and (d) with the red arrows indicating the flow direction. (For interpretation of the references to colour in this figure legend, the reader is referred to the web version of this article).

to the gap at the absorption peak frequencies. Fig. 4(c) and (d) show the corresponding surface current with red arrows indicating the direction. These results reveal that LC resonance is excited for parallel polarization, while dipole resonance is excited for perpendicular polarization.

The electric field distribution of the LC and dipole absorption modes were further investigated to obtain a comprehensive understanding of the air-spacer absorber. Fig. 5(a) and (b) depict the electric field distributions of the two absorption modes at the cross sections (shown as the insets), parallel or perpendicular to the capacitive gap. For the LC absorption mode, the electric field is primarily perpendicular to the ground plane, but is parallel to the ground plane in the gap. For the dipole absorption mode, the electric field below the metamaterial structure is also perpendicular to the ground plane. However, the electric field at the boundaries is much stronger than that of the LC absorption mode, which indicates stronger coupling between unit cells. The simulated electric field strength at the cross section at the midpoint of the spacer in x–y cross section is depicted in Fig. 5(c) and (d) for LC and dipole absorption modes. The maximum strength occurs at the sides labeled 5 and 6 (as labeled in Fig. 4(c)) forming the gap for the LC absorption mode, while minimum strength occurs at the sides labeled 1 and 2 parallel to the gap. In the case of the dipole mode, the maximum strength occurs at the sides labeled 1 and 2, while minimum strength occurs at the sides labeled 5 and 6. Nevertheless, both LC and dipole absorption modes exhibited high electric field concentration inside the spacer volume, particularly underneath the SRRs, indicating that the absorption should be very sensitive to the spacer permittivity.

In principle, for the air-spacer absorber, it should be possible to modify the permittivity using, for example, microfluidics. This could change the absorption strength and frequency of the resonance. Given the reasonably high quality factor, this gives the air-spacer metamaterial absorber a unique set of advantages for potential sensing applications. In the following, we investigate this possibility using simulations to motivate future work along these lines. Fig. 6(a) depicts the simulated absorption spectra by changing the imaginary part of the spacer permittivity ε_i (where the permittivity is $\varepsilon = \varepsilon_r + i\varepsilon_i$) with ε_r held constant. The increasing loss lowers the quality factor and decreases the absorption. However, the absorption peak frequency remains nearly constant. Fig. 6(b) shows the absorption spectra obtained upon changing ε_r of the spacer permittivity with ε_i held constant. The absorption peak frequency red shifts with increasing ε_r caused by a larger capacitance, with minimal change in the quality factor. However, we note that the thin fragile silicon nitride membrane is critical to achieve the high sensitivity [23] and has to be carefully handled when designing such a sensor.

4. Conclusion

In summary, we designed, fabricated, and characterized an air-spaced terahertz metamaterial absorber. Due to the absence of the dielectric loss, the quality factor is increased by greater

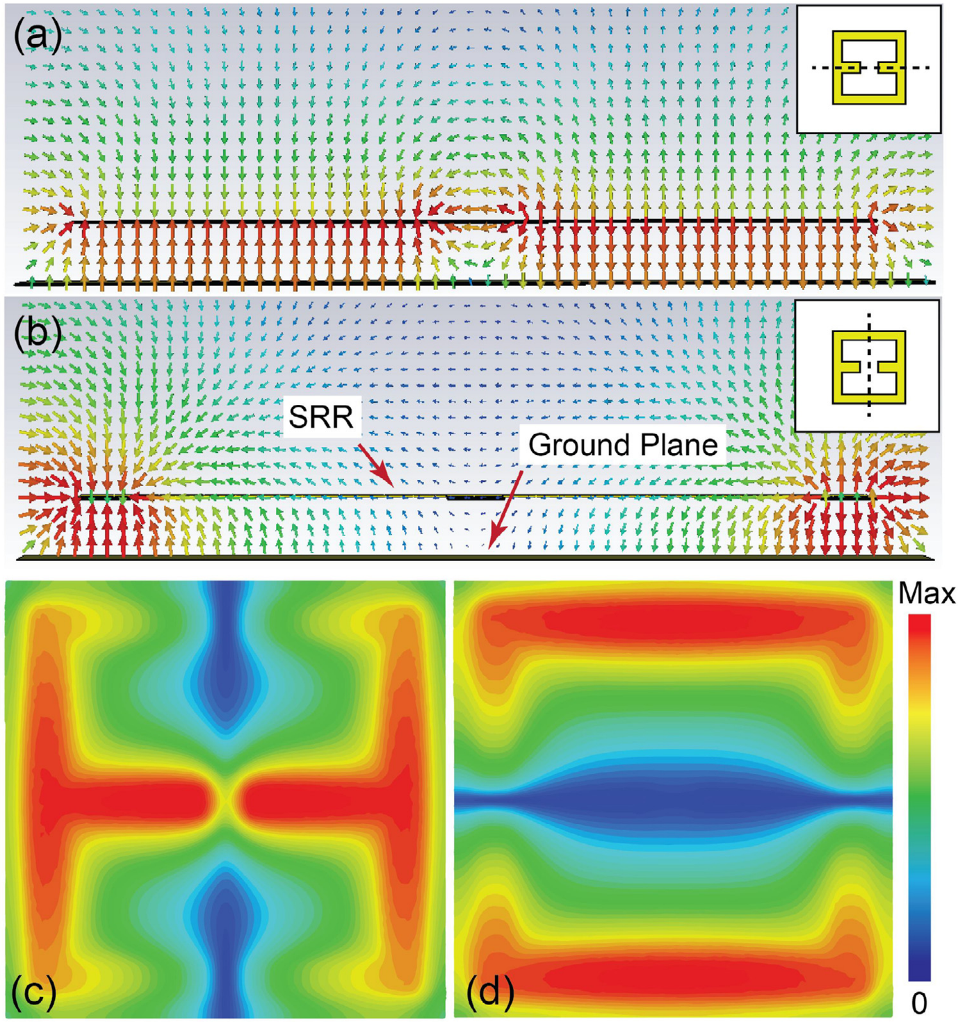

Fig. 5. (a) The electric field distribution for the LC absorption mode in the x–z cross section at the position depicted by the dashed line in the inset. (b) The electric field distribution for the dipole absorption mode in the y–z cross section. The electric field strength at the middle of the spacer in x–y cross section for (c) LC and (d) dipole absorption modes.

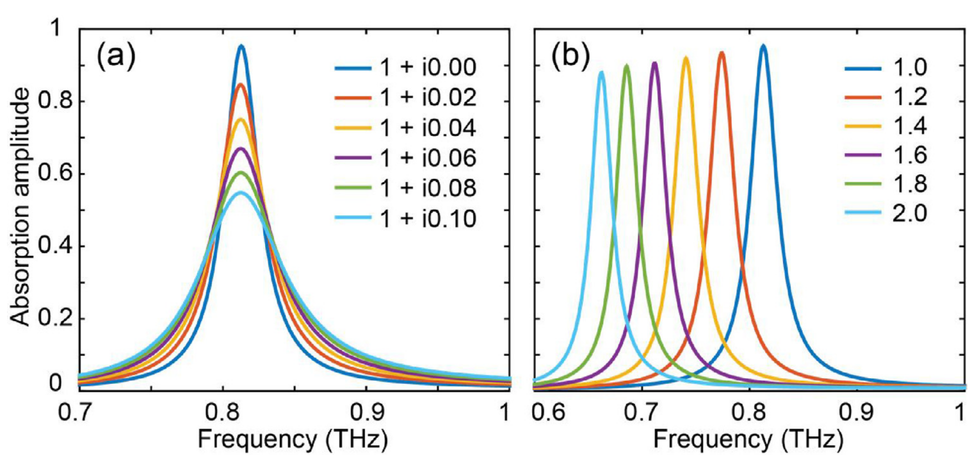

Fig. 6. The simulated absorption spectra with different spacer permittivity. (a) Varying the imaginary part with identical real part as 1. (b) Varying the real part with identical imaginary part as zero.

than three-fold when compared to conventional metamaterial perfect absorbers. Further increases in the quality factor are limited because of losses in the metallic layers. Simulations of the local electric fields reveal that the electric field is highly concentrated between the two metallic layers, especially beneath the SRRs. With additional effort to create a mechanically robust air-spaced absorber, such a device can potentially be utilized for dielectric sensing applications.

Acknowledgements

This work was supported by the National Science Foundation [grant number ECCS-1309835]; DOE - Basic Energy Sciences [grant number DE-SC0018218]. The authors would like to thank Boston University Photonics Center for technical support.

References

[1] D.R. Smith, W.J. Padilla, D.C. Vier, S.C. Nemat-Nasser, S. Schultz, Composite medium with simultaneously negative permeability and permittivity, Phys. Rev. Lett. 84 (2008) 4184.
[2] D.R. Smith, J.B. Pendry, M.C.K. Wiltshire, Metamaterials and negative refractive index, Science 305 (2004) 788–792.
[3] X. Zhao, K. Fan, J. Zhang, G.R. Keiser, G. Duan, R.D. Averitt, X. Zhang, Voltage-tunable dual-layer terahertz metamaterials, Microsyst. Nanoeng.–Nat. 2 (2016) 16025.
[4] N.I. Landy, S. Sajuyigbe, J.J. Mock, D.R. Smith, W.J. Padilla, Perfect metamaterial absorber, Phys. Rev. Lett. 100 (2008), 207402.
[5] H. Tao, N.I. Landy, C.M. Bingham, X. Zhang, R.D. Averitt, W.J. Padilla, A metamaterial absorber for the terahertz regime: design, fabrication, and characterization, Opt. Express 16 (2008) 7181–7188.
[6] H. Tao, C.M. Bingham, A.C. Strikwerda, D. Pilon, D. Shrekenhamer, N.I. Landy, K. Fan, X. Zhang, W.J. Padilla, R.D. Averitt, Highly flexible wide angle of incidence terahertz metamaterial absorber: design, fabrication, and characterization, Phys. Rev. B 78 (2008), 241103(R).
[7] F. Costa, A. Monorchio, G. Manara, Analysis and design of ultra thin electromagnetic absorber comprising resistively loaded high impedance surfaces, IEEE Trans. Antennas Propag. 59 (2010) 1551–1558.
[8] B.A. Munk, P. Munk, J. Pryor, On designing Jaumann and circuit analog (CA absorbers) for oblique angle of incidence, IEEE Trans. Antennas Propag. 55 (2007) 186–193.
[9] F. Costa, S. Genovesi, A. Monorchio, G. Manara, A circuit-based model for the interpretation of perfect metamaterial absorbers, IEEE Trans. Antennas Propag. 6 (2013) 1201–1209.
[10] Q. Wen, Y. Xie, H. Zhang, Q. Yang, Y. Li, Y. Liu, Transmission line model and fields analysis of metamaterial absorber in the terahertz band, Opt. Express 17 (2009) 20256–20265.
[11] H.-T. Chen, Interference theory of metamaterial perfect absorbers, Opt. Express 20 (2012) 7165–7172.
[12] N.I. Landy, C.M. Bingham, T. Tyler, N. Jokerst, D.R. Smith, W.J. Padilla, Design, theory, and measurement of a polarization-insensitive absorber for terahertz imaging, Phys. Rev. B 79 (2009), 125104.
[13] N. Liu, M. Mesch, T. Weiss, M. Hentschel, H. Giessen, Infrared perfect absorber and its application as plasmonic sensor, Nano Lett. 10 (2010) 2342–2348.
[14] D. Shrekenhamer, W. Chen, W.J. Padilla, Liquid crystal tunable metamaterial absorber, Phys. Rev. Lett. 110 (2013), 177403.
[15] M.J. Dicken, K. Aydin, I.M. Pryce, L.A. Sweatlock, E.M. Boyd, S. Walavalkar, J. Ma, H.A. Atwater, Frequency tunable near-infrared metamaterials based on VO_2 phase transition, Opt. Express 17 (2009) 18330–18339.
[16] X. Zhao, J. Zhang, K. Fan, G. Duan, G.D. Metcalfe, M. Wraback, X. Zhang, R.D. Averitt, Nonlinear terahertz metamaterial perfect absorbers using GaAs, Photonics Res. 4 (2016) A16–A21.
[17] G. Cataldo, J.A. Beall, H. Cho, B. McAndrew, M.D. Niemack, E.J. Wollack, Infrared dielectric properties of low-stress silicon nitride, Opt. Lett. 37 (2012) 4200–4202.
[18] G. Duan, J. Schalch, X. Zhao, J. Zhang, R.D. Averitt, X. Zhang, An air-spacer terahertz metamaterial perfect absorber for sensing and detection applications, in: Solid-State Sensors, Actuators and Microsystems (Transducers) 19th International Conference on, 2017, pp. 1999–2002.
[19] S.A. Tretyakov, Dynamic model of artificial reactive impedance surfaces, J. Electromagn. Waves Appl. 17 (2003) 131–145.
[20] L. Huang, D.R. Chowdhury, S. Ramani, M.T. Reiten, S. Luo, A.K. Azad, A.J. Taylor, H.-T. Chen, Impact of resonator geometry and its coupling with ground plane on ultrathin metamaterial perfect absorbers, Appl. Phys. Lett. 101 (2012), 101102.
[21] C.M. Watts, X. Liu, W.J. Padilla, Metamaterial electromagnetic wave absorbers, Adv. Opt. Mater. 24 (2012) OP98–OP120.
[22] H.R. Seren, G.R. Keiser, L. Cao, J. Zhang, A.C. Strikwerda, K. Fan, G.D. Metcalfe, M. Wraback, X. Zhang, R.D. Averitt, Optical modulated multiband terahertz perfect absorber, Adv. Opt. Mater. 2 (2012) 1221–1226.
[23] H. Tao, A.C. Strikwerda, M. Liu, J.P. Mondia, E. Ekmekci, K. Fan, D.L. Kaplan, W.J. Padilla, X. Zhang, R.D. Averitt, F.G. Omenetto, Performance enhancement of terahertz metamaterials on ultrathin substrates for sensing applications, Appl. Phys. Lett. 97 (2010), 261909.

Biographies

Guangwu Duan received his B.S. and M.S. degree from Xi'an Jiaotong University, Xi'an, China and Tsinghua University, Beijing, China in 2008 and 2010, respectively. He is currently pursuing the Ph.D. degree at the Department of Mechanical Engineering, Boston University, Boston, MA, USA. His research interests include Micro Electro-Mechanical Systems (MEMS) design and fabrication, RF communication, wireless power transfer, and Terahertz metamaterials.

Jacob Schalch is currently pursuing the Ph. D. degree at the Department of Physics, University of California San Diego, La Jolla, California.

Xiaoguang Zhao received the Ph.D. degree in Mechanical Engineering from Boston University, Boston, MA, USA, in 2016, and the M.E. degree from Tsinghua University, Beijing, China, in 2011. His research interests include micro-electromechanical systems (MEMS) design and fabrication, RF communications, and terahertz and infrared metamaterial devices.

Jingdi Zhang received the Ph.D. degree in Physics from Boston University, Boston, MA, USA, in 2014. He is currently a postdoctoral researcher at the Department of Physics, University of California at San Diego, La Jolla, CA, USA. His research interests include ultrafast spectroscopy of strongly correlated materials, metamaterials and light-control (visible to far-infrared) of transition metal oxides.

Richard D. Averitt received the Ph.D. degree in applied physics from Rice University, Houston, TX, USA, in 1998. Following this, he was a Los Alamos National Laboratory Directors Post-Doctoral Fellow. His postdoctoral work focused on time-resolved far-infrared spectroscopy of strongly correlated electron materials. In 2001, he became a Member of the Technical Staff with Los Alamos National Laboratory, Los Alamos NM, USA and in 2005, a member of the Center for Integrated Nanotechnologies co-located at Los Alamos and Sandi a National Laboratories. In 2007, he joined Boston University, Boston, MA, USA, as a Faculty Member with the Department of Physics and the Boston University Photonics Center. Since 2014, he has been a Professor with the Department of Physics, University of California at San Diego, La Jolla CA, USA. His research interests are primarily directed towards characterizing the optical and electronic properties of materials including metamaterials and plasmonic composites, quantum cheese, transition metal oxides, and other complex materials using experimental techniques which span from the far-infrared through the visible.

Xin Zhang received the Ph.D. degree in mechanical engineering from the Hong Kong University of Science and Technology, Hong Kong, in 1998. She was a Post-Doctoral Researcher and then a Research Scientist with the Massachusetts Institute of Technology, Cambridge, MA, USA, from 1998 to 2001. She then joined Boston University, Boston, MA, USA, as a Faculty Member, where she is currently a Professor with the Department of Mechanical Engineering, the Division of Materials Science and Engineering, and the Boston University Photonics Center. Her research interests are in the fundamental and applied aspects of micro/nanoelectromechanical systems. In particular, she seeks to understand and exploit interesting characteristics of micro/nanomaterials, micro/nanomechanics, and micro/nanomanufacturing technologies with forward-looking engineering efforts and practical applications ranging from energy to health care to homeland security. In 2009, she was named the inaugural Distinguished Faculty Fellow, an honor given to tenured College of Engineering faculty at Boston University who is on a clear trajectory toward exemplary leadership career in all dimensions of science and engineering. In 2016, she was selected as the recipient of the IEEE Sensors Council Technical Achievement Award in the area of Sensors (advanced career) for distinguished contributions to the field of micro/nanoelectromechanical systems. Dr. Zhang is a Fellow of AAAS, AIMBE, ASME, IEEE, and OSA.